Gyrokinetic investigation of the nonlinear interplay of Alfvén instabilities and energetic particles in tokamaks.

A. Biancalani[1], M. Cole[2] A. Bottino[1], A. Könies[2], Ph. Lauber[1], A. Mishchenko[2], Z. Qiu[3], B. Scott[1], F. Zonca[4,3]

[1]Max-Planck-Institut für Plasmaphysik, 85748 Garching, Germany

[2]Max-Planck-Institut für Plasmaphysik, 17491 Greifswald, Germany

[3]Institute for Fusion Theory and Simulation, Zhejiang University, Hangzhou, P. R. China

[4]ENEA C. R. Frascati, C.P. 65-00044 Frascati, Italy

Contact of main author: www2.ipp.mpg.de/~biancala

Abstract. Alfvén Eigenmodes (AE) are global instabilities excited by energetic particles (EP) in magnetic fusion devices. AE can redistribute the EP population across flux surfaces, making the plasma heating less effective, and leading to additional loads on the walls. The interplay of AEs and EPs is investigated by means of gyrokinetic particle-in-cell simulations, with a nonperturbative approach. The global nonlinear codes ORB5 and EUTERPE are used for such studies. Both wave-particle and wave-wave nonlinearities are considered and various aspects of the nonlinear dynamics are addressed separately, by artificially switching off other nonlinearities. When concentrating on the wave-particle nonlinearity, a detailed study of the saturation is performed, as a consequence of the redistribution of the EP population in phase-space. A comparison with GK-MHD hybrid codes is also presented. When allowing wave-wave nonlinearities to occur with a zonal structure, the saturation level of the AE is observed to be drastically reduced. As a consequence, a much lower redistribution of EP is observed with respect to the case where only the wave-particle nonlinearity is allowed. Finally, numerical simulations of multiple modes with different toroidal mode number are also presented.

1. Introduction

In magnetic fusion devices, the energetic particle (EP) population due to plasma heating, together with alpha particles produced in fusion reactions, excite plasma oscillations via resonant wave-particle interactions. On the other hand, plasma instabilities such as Alfvén Eigenmodes (AEs) can redistribute the EP population across flux surfaces, making the plasma heating less effective, and leading to additional loads on the walls [1, 2]. Toroidicity-induced AEs (TAEs) [1] are considered to be among the most efficient AEs in redistributing the EP population in ITER [3]. For this reason, international benchmark efforts have been made in order to assess a level of trustability of the computational understanding of their dynamics. The International Tokamak Physics Activity (ITPA) benchmark has started by focusing on the linear dynamics of TAEs, and comparing the results of several gyrokinetic (GK), gyrofluid, and hybrid GK-MHD codes [4]. Numerically, a good level of understanding of the wave-particle interaction in the linear and nonlinear phase of the TAEs growth has been recently achieved by means of hamiltonian mapping diagnostics [5]. Analytically, a unified approach for weakly and strongly driven AEs and energetic-particle driven continuum modes (EPMs) [6] has been derived, based on a generalized fishbone-like dispersion relation (GFLDR), which helps extracting the underlying physics of the numerical simulations [7].

Plasmas in magnetic fusion devices are turbulent. Thereby, turbulence brings in an additional twist to the EP-redistribution problem. Consistently, wave-wave coupling of turbulence and zonal structures - such as zero-frequency zonal flows (ZF) [8, 9] and finite-frequency geodesic acoustic modes (GAM) [10, 11] - with AEs competes with wave-particle nonlinear interaction

as saturation mechanisms of AEs. The nonlinear interaction of zonal structures and AEs has been recently analytically derived for both force-driven and parametrically excited ZFs [12]. For these reasons, it is important to develop a proper selfconsistent theoretical framework for understanding the nonlinear interplay (generally non-perturbative) of AEs, EPs and turbulence in present tokamaks and predict the implications in future fusion reactors. The GK formalism has been proved to be a robust framework for such a development, due to the nice properties of conservation of energy and momentum [13].

2. The theoretical models

In this work, we investigate the interplay of AEs and EP by means of GK particle-in-cell simulations. Electromagnetic GK simulations require a robust self-consistent model and a robust numerical discretisation, mainly due to the kinetic treatment of the electrons (crucial for a proper treatment of Alfvénic and acoustic modes). This level of accuracy has been recently achieved with the codes ORB5 and EUTERPE. The global nonlinear code ORB5, originally developed for electrostatic turbulence studies [14], has been recently extended to electromagnetic within the NEMORB project [15, 16, 17]. Due to the method of derivation of the GK Vlasov-Maxwell equations from a discretized Lagrangian, the symmetry properties of the starting Lagrangian are passed to the Vlasov-Maxwell equations, and the conservation theorems for the energy and momentum are automatically satisfied [18]. Recently, a detailed linear verification and benchmark of ORB5 on AEs has been performed [19]. EUTERPE [20] is a global nonlinear code that models the ions and electrons either as GK species or as a fluid [21], providing insights into the AE underlying physics processes. The model equations of EUTERPE, similar in origin to those of ORB5, are implemented in a mixed-variable-formulation [22, 23]. EUTERPE adopts general 3D equilibria, and it is therefore particularly suited for studies in non-axisymmetric geometries like stellarators.

3. ITPA-TAE case

3.1. Equilibrium

The equilibrium of the International Tokamak Physics Activity (ITPA) [4, 19] is considered for the studies of nonlinear dynamics of the TAE with toroidal mode number n=6. The major radius and minor radius are $R_0 = 10$ m and $a = 1$ m. The toroidal magnetic field is $B_0 = 3$ T, and the safety factor is $q(r) = 1.71 + 0.16(r/a)^2$. The bulk ion is chosen to be hydrogen. The ion and electron average densities are $n_i = n_e = 2 \cdot 10^{19} \mathrm{m}^{-3}$. In the case of a nonuniform profile of an additional species (for example of the EP), the bulk ion and electron profiles are corrected in order to satisfy quasi-neutrality, as described below. The bulk ion and electron temperature is $T_i = T_e = 1$ keV. The corresponding bulk ion cyclotron frequency is $\Omega_i = 2.87 \cdot 10^8$ rad/s, the electron beta on axis is $\beta_e = 8\pi n_e T_e / B_0^2 = 8.955 \cdot 10^{-4}$ and the Alfvén velocity on axis is $v_A = 1.46 \cdot 10^7$ m/s.

Given these parameters, we can calculate the continuous spectrum near the toroidicity induced gap of the TAE. The X-point where the two cylinder continuum branches cross (neglecting toroidicity and compressibility) is located at $\omega_{CXP} = v_A/2qR_0 = 1.454 \cdot 10^{-3}\Omega_i$. The continuum accumulation points can be calculated by using the approximated formula given in Ref. [19] (derived after Ref. [1, 24]), valid for small values of inverse aspect ratio. We obtain

that the lower continuum accumulation point (LCAP) calculated with compressibility effects, is located at $\omega_{LCAP} \simeq 1.43 \cdot 10^{-3}\Omega_i$ and the upper continuum accumulation point (UCAP) at $\omega_{UCAP} \simeq 1.54 \cdot 10^{-3}\Omega_i$ (the upshift due to the compressibility effect, calculated as in Ref. [26], is $\simeq 0.03 \cdot 10^{-3}\Omega_i$). A global AE with frequency at $\omega = 1.435 \cdot 10^{-3}\,\Omega_i$ is observed when a perturbation is let evolve in the absence of EP.

A distribution function Maxwellian in velocity-space is considered for the EP population. The EP averaged concentration of a reference case is $\langle n_{EP}\rangle/n_e = 0.004$ with radial profile given by $n_{EP}(s)/n_{EP}(s_0) = \exp[-\Delta\,\kappa_n\tanh((s - s_0)/\Delta)]$ with $s_0 = 0.5$, $\Delta = 0.2$, and $\kappa_n = 3.333$. When the EP ion species is added, the total number of electrons in the volume is kept the same, and the bulk ion average concentratoin is diminished in order for the total number of ions (bulk plus energetic) to equal the total number of electrons. The bulk ion and electron profiles are kept flat in the simulations used here (like in Ref. [19]). The reference EP temperature in this paper is $T_{EP} = 500$ keV (like in Ref. [19]). For consistency with Ref. [19], no FLR effects are retained in the simulations shown in this paper. This means that the Bessel functions are calculated for vanishing argument. The investigation of the FLR effects will be done in a separate paper.

3.2. Nonlinear saturation via wave-particle interaction

In this section, we describe the result of simulations where the wave-particle nonlinearity only is considered. This is achieved by pushing the bulk ions and electrons along the unperturbed trajectories, and the EP along the perturbed trajectories. After a linear phase ($t < 2 \cdot 10^4$) the mode amplitude, measured as the maximum of the vector potential A in the poloidal plane, is observed to enter a "drift-phase" (see Fig. *1.*), characterized by a slower subexponential growth ($2 \cdot 10^4 < t < 8 \cdot 10^4$), and then a saturation ($t > 8 \cdot 10^4$) . The EP profile is observed to start redistributing during the drift phase. The saturation levels of the poloidal component of the magnetic field can be measured for different values of the EP concentration. The scalings, obtained with different models, are shown in Fig. *2.*. A good qualitative agreement in the scaling is found for GK and hybrid models. As for the absolute value of the levels, a good agreement between the GK models is found, whereas models not accounting for the electron damping, and assuming an artificial damping, show a lower saturation level [28].
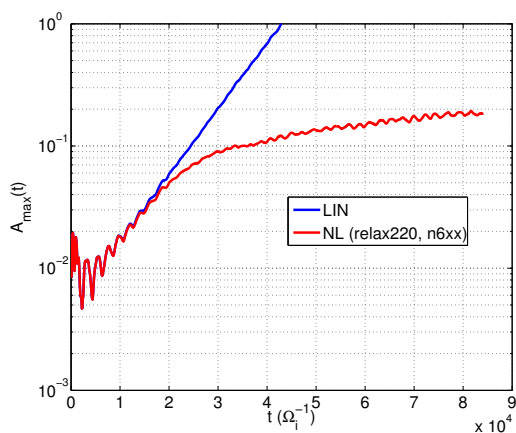

FIG. 1.: Maximum of the vector potential with ORB5 for the linear and nonlinear ITPA-TAE with $n_{EP}/n_e = 0.0031$, $T_{EP}/T_e = 500$.
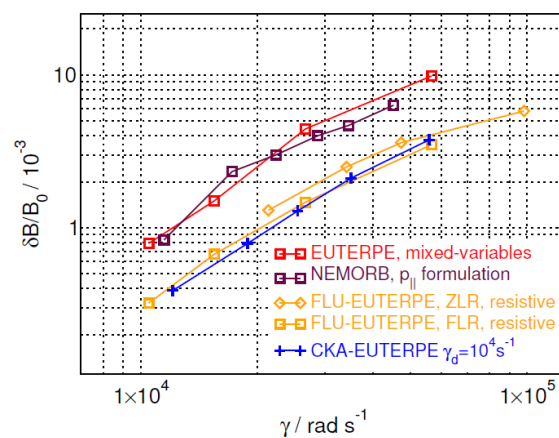
FIG. 2.: Saturation levels vs growth rates, obtained with different models, for the ITPA-TAE [28].

3.3. Nonlinear structure modification

During the drift phase due the wave-particle nonlinearity, the radial width of the TAE mode becomes smaller. This is found to be due in part to the decrease of the density gradient and in part to the redistribution of the EP population in velocity space. During the saturation phase, no difference is found in the main mode structure, except for small perturbations being observed radially [29].
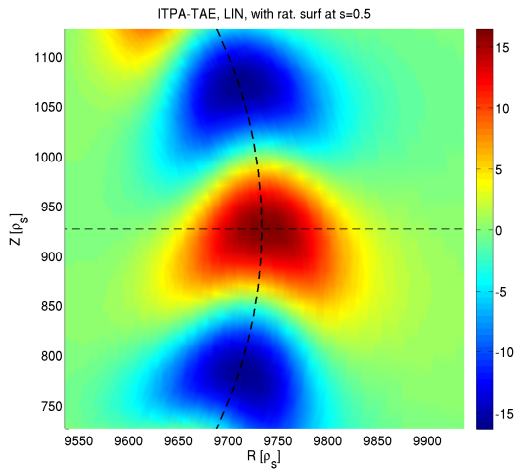

FIG. 3.: Scalar potential ϕ in the linear phase of the ITPA-TAE, for $n_{EP}/n_e = 0.004$, $T_{EP}/T_e = 400$.
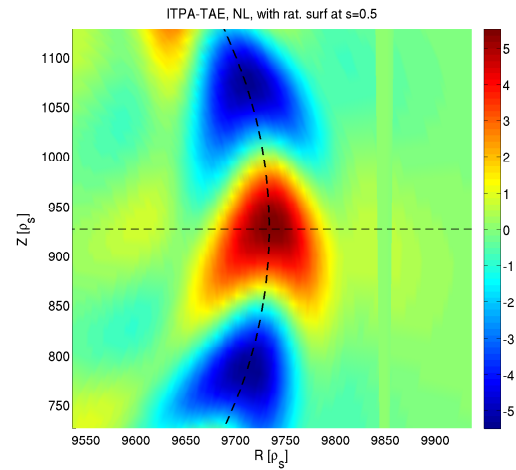
FIG. 4.: Scalar potential ϕ in the nonlinear phase of the ITPA-TAE, for $n_{EP}/n_e = 0.004$, $T_{EP}/T_e = 400$.

3.4. Nonlinear saturation via wave-particle and wave-wave interaction

Simulations with the ITPA-TAE equilibrium have been also performed where two TAEs are allowed to evolve: one with n=2 and one with n=6. The hybrid code FLU-EUTERPE [21] has been used for these simulations, where electrons are treated as fluid, in the ITPA equilibrium with $T_{EP}/T_e = 400$ keV. In Fig. 5., two simulations are shown. When the wave-particle nonlinearity only is considered, the most unstable mode, namely the n=2 TAE, is observed. On the other hand, when wave-wave coupling is also included, the n=2 mode is shown to grow in a shorter linear phase, after which it couples to the n=6 and saturates earlier than the case where wave-particle nonlinearity only was considered [28].
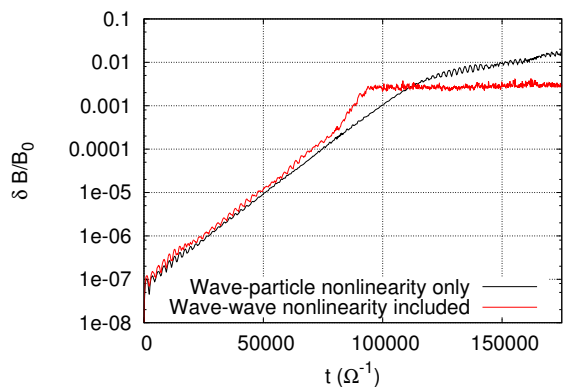

FIG. 5.: TAEs with n=2 and n=6 studied with FLU-EUTERPE for the ITPA equilibrium, with wave-particle nonlinearity only (black line), and with wave-wave nonlinearity included (red line) [28].

4. Continuum mode with flat q-profile

4.1. Equilibrium

The equilibrium magnetic field and the equilibrium density and temperature profiles assumed here are the same ones as in Ref. [19], where continuum modes are studied in the linear regime. The magnetic equilibrium is the same analytical equilibrium as in the previous sections, with same magnetic field intensity at the axis (B=3T), but with a different poloidal component, yielding a flat safety factor profile, with $q(\rho = 0.5)$=1.78. Ion and electron density and temperature profiles are flat, with $T_i = T_e$=55.1 keV (corresponding to $\rho^* = 1/125$). The electron pressure is chosen for a value of $\beta_e = 5 \cdot 10^{-4}$. The mode frequency in the limit of zero EP concentration tends to the continuum frequency, therefore we refer to these modes as EP driven continuum modes (EPM) [6]. We note that this equilibrium is greatly simplified with respect to a realistic tokamak equilibrium. This is chosen on purpose to have a test case where the zonal structures are more visible. As a consequence, the results obtained in this equilibrium have no direct quantitative implications in the dynamics of realistic tokamak scenarios.

4.2. Frequency spectra

In a simulation where both a continuum mode and a zonal structure are allowed to develop (whereas all other toroidal mode numbers are filtered out), two main frequencies can be measured. One frequency is measured by performing a Fourier transform of the vector potential measured in one point in space: this is shown to fall near the shear-Alfvén continuum spectrum, and it is therefore the frequency of the Alfvén continuum mode (see Fig. 6.). When performing the Fourier transform on the zonal component (m=0, n=0) of the radial electric field, we observe a finite frequency near the analytical prediction for the GAM frequency, and a much lower frequency at larger radii: this identifies a GAM and a zero-frequency zonal flow (see Fig. 7.).
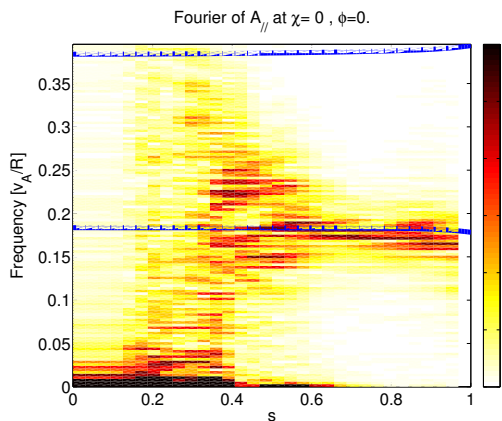

FIG. 6.: *Fourier transform in time of the vector potential measured in one point in space, corresponding to the continuum mode oscillation.*
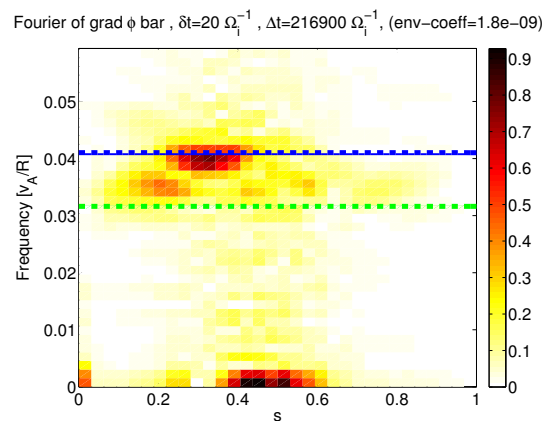
FIG. 7.: *Fourier transform in time of the zonal radial electric field, corresponding to the zonal structure.*

4.3. Nonlinear saturation via wave-particle and wave-wave interaction

For the ITPA-TAE, we have focused on the wave-particle nonlinearity and with wave-wave interaction of n=2 and n=6 TAEs. Here, we investigate two mechanisms which can compete:
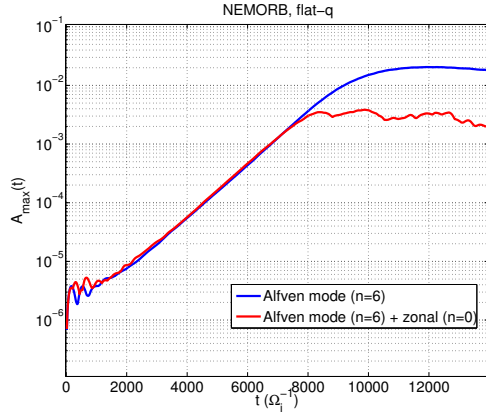
FIG. 8.: *Vector potential measured at $s = 0.5$, $\chi = 0$, for the linear simulation, the nonlinear simulation with only the continuum mode with n=6, and the nonlinear simulation with both n=6 and n=0.*
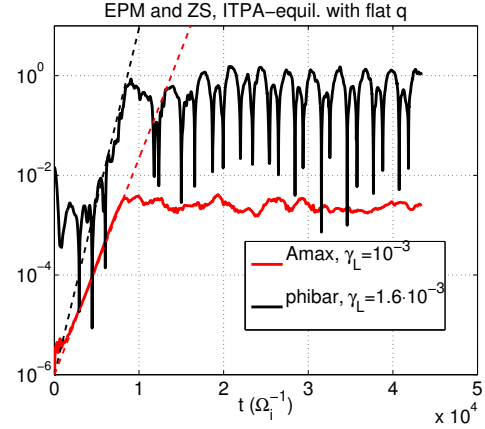
FIG. 9.: *Evolution of the vector potential measured in one point, corresponding to the Alfvén continuum mode (red line) and of the zonal Fourier component of the scalar potential, corresponding to the zonal structure (black line).*

one is the redistribution of the EP population in phase space, which occurs due to the wave-particle nonlinearity, and the other is the generation of a zonal structure. In the case when the zonal structure is allowed to develop, the continuum mode saturation level is measured to be about one order of magnitude lower (see Fig. *8.*). The zonal structure is observe to develop already during the linear phase of the continuum mode growth, with a constant growth rate $\gamma_z \simeq 1.6\gamma_A$ (see Fig. *9.*). This identifies the driving mechanism of the zonal structure as a parametric excitation (see Ref. [12], where the ratio of the growth rates is calculated in a different regime, corresponding to the interaction of a TAE and a zonal structure).

4.4. EP radial redistribution

In an equilibrium with flat q profile the EP radial redistribution can be observed very clearly due to the relatively big radial structure of the continuum mode. In the simulation where only the Alfvén mode is allowed to develop, a clear decrease in the EP radial density gradient is observed (see Fig. *10.*). On the other hand, due to the lower saturation level, the continuum
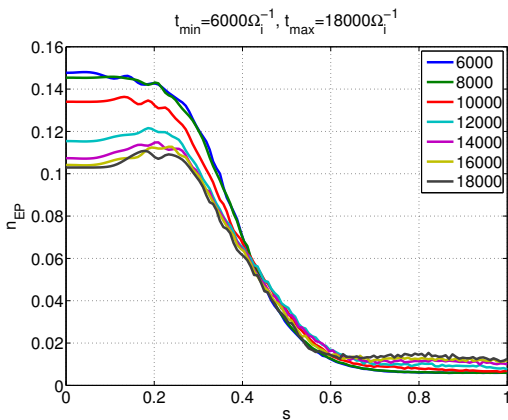

FIG. 10.: *EP radial redistribution in time for a simulation where only the continuum mode is kept.*
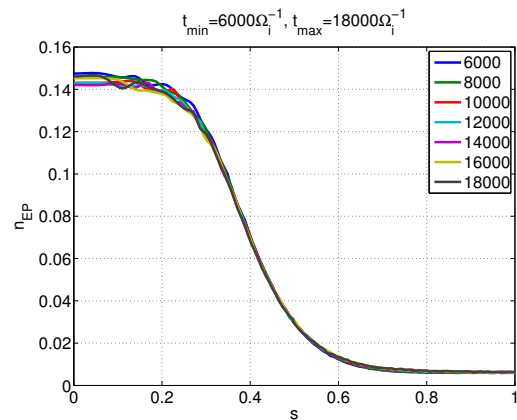
FIG. 11.: *EP radial redistribution in time for a simulation where both the continuum mode (n=6) and the zonal structure (n=0) are kept.*

mode does not redistribute the EP radially, when the energy is absorbed by the zonal structure (see Fig. *11.*).

5. Conclusions

The nonlinear dynamics of AEs has been investigated here with a nonperturbative approach, namely allowing the mode radial structure and EP profile to evolve in a selfconsistent way. Alfvén modes such as toroidicity-induced AE (TAE) of the International Tokamak Physics Activity and fluctuations of the continuum, near a radial region with vanishing magnetic shear, have been considered. The nonlinear interplay of mode structure and energetic particle transport has been systematically investigated and explained. In particular, both wave-particle and wave-wave nonlinearities have been considered and various aspects of the nonlinear dynamics have been addressed separately, by artificially switching off other nonlinearities.

When concentrating on the wave-particle nonlinearity, a detailed study of the saturation level has been performed by filtering out all but the toroidal mode number n=6, and focusing on the EP interaction with a single Alfvén mode (see also Ref. [23]). It is found, for this particular case, that hybrid models treating the electrons as fluid, underestimate the saturation level with respect to gyrokinetic models. Part of this difference is thought to depend on the value of the artificial damping needed for hybrid models to achieve the saturation phase (not necessary with the GK models). The mode structure has also found to shrink at the beginning of the nonlinear phase, consistently with simulations shown in Ref. [30], and consistently with what observed experimentally for EPMs [31].

When studying the wave-wave nonlinearity, one extra non-zonal mode [28] or zonal mode [29] can be allowed to develop, interacting nonlinearly with the EP population and with the main mode. A simplified equilibrium, with flat q-profile, has been considered in order to emphasize this excitation (and therefore this has no quantitative implications on realistic tokamak scenarios). Zonal structures such as ZF and GAM are observed to develop as a competition of Maxwell and Reynolds stress nonlinearity and curvature coupling effects. This is consistent with what observed numerically in hybrid codes [32, 33] and derived analytically [12]. The saturation level of Alfvén mode in these cases is observed to be drastically reduced. This can be due to the Landau damping which acts more efficiently on the GAM than on the (higher frequency) Alfvén mode, and therefore acts as an energy sink, or to the EP redistribution in phase space, which modifies the resonance frequency. As a consequence, a much lower radial redistribution of EP is observed with respect to the case where only the wave-particle nonlinearity is allowed.

6. Acknowledgments

References

[1] C. Z. Cheng, L. Chen, and M. S. Chance, *Ann. Phys* **161**, 21 (1985)

[2] L. Chen and F. Zonca, *Rev. Mod. Phys.* **88**, 015008 (2016)

[3] M. Schneller, et al *Plasma Phys. Control. Fusion* **58**, 014019 (2016)

[4] A. Köenies, et al, "Benchmark of gyrokinetic, kinetic MHD and gyrofluid codes for the linear calculation of fast particle driven TAE dynamics", IAEA-FEC, ITR/P1-34 (2012)

[5] S. Briguglio, et al., *Phys. Plasmas* **21**, 112301 (2014)

[6] L. Chen, F. Zonca, *Nucl. Fusion* **47** S727 (2007)

[7] F. Zonca and L. Chen, *Phys. Plasmas* **21** 072121 (2014)

[8] A. Hasegawa, et al., *Phys. Fluids* **22**, 2122 (1979)

[9] P. H. Diamond, et al., *Plasma Phys. Controlled Fusion* **47**, R35 (2005)

[10] N. Winsor, et al. *Phys. Fluids* **11**, 2448 (1968)

[11] F. Zonca and L Chen, *Europhys. Lett.* **83**, 35001 (2008)

[12] Z. Qiu, et al, *Phys. Plasmas*, in press (2016)

[13] B. D. Scott, and J. Smirnov *Phys. Plasmas* **17**, 112302 (2010)

[14] S. Jolliet, et al, *Comput. Phys. Commun.* **177**, 409 (2007)

[15] A. Bottino, *Plasma Phys. Controlled Fusion* **53**, 124027 (2011)

[16] N. Tronko, A. Bottino, and E. Sonnendrücker, *Phys. Plasmas* **23**, 082505 (2016)

[17] A. Biancalani, et al. "Adapting a gyrokinetic global code for Alfvén modes", *to be submitted to Comput. Phys. Commun.* (2016)

[18] A. Bottino and E. Sonnendrücker, *J. Plasma Phys.* **81**, 435810501 (2015)

[19] A. Biancalani, et al, 2016 *Phys. Plasmas* **20** 012108

[20] Kornilov V., et al., 2004 *Phys. Plasmas* 11, 3196

[21] M. Cole, et al., 2015 *Plasma Phys. Control. Fusion* 57, 054013

[22] A. Mishchenko, A. Könies, R. Kleiber, and M. Cole, *Phys. Plasmas* **21**, 092110 (2014)

[23] Cole M. D. J., et al., *submitted to Phys. Plasmas* (2016)

[24] G. Y. Fu and J. W. Van Dam, *Phys. Fluids* **B 1**, 1949 (1989)

[25] A. Mishchenko, et al, Nucl. Fusion **55** 053006 (2015)

[26] F. Zonca, L. Chen and R.A. Santoro *Plasma Phys. Control. Fusion* **38**, 2011-2028 (1996)

[27] F. Zonca and L. Chen, *Phys. Rev. Lett.* **68**, 5, 592 (1992)

[28] M. Cole, et al., *IAEA Technical Meeting on Energetic Particles in Magnetic Confinement Systems, September 1 - 4 2015, Vienna, Austria*, I12 (2015)

[29] A. Biancalani, et al, 2015 *IAEA Technical Meeting on Energetic Particles in Magnetic Confinement Systems, September 1 - 4 2015, Vienna, Austria*, I7

[30] A. Biancalani, et al, *to be submitted to Plasma Phys. Control. Fusion* (2016)

[31] L. Horváth, et al, *Nucl. Fusion* **56**, 112003 (2016).

[32] Y. Todo, et al, *Nucl. Fusion* **50**, 084016 (2010).

[33] H. Zhang, and Z. Lin, *Plasma Sc. and Tech.* **15** 969 (2013).